Transfer matrix method for solution of FGMs thick-walled cylinder with arbitrary inhomogeneous elastic response

Y.Z. Chen*

Division of Engineering Mechanics, Jiangsu University, Zhenjiang, Jiangsu, 212013 P. R. China

Abstract. This paper presents a numerical solution for the thick cylinders made of functionally graded materials (FGMs) with a constant Poisson's ratio and an arbitrary Young's modulus. We define two fundamental solutions which are derived from an ordinary differential equation under two particular initial boundary conditions. In addition, for the single layer case, we can define the transfer matrix **N**. The matrix gives a relation between the values of stress and displacement at the interior and exterior points. By using the assumed boundary condition and the transfer matrix, we can obtain the final solution. The transfer matrix method also provides an effective way for the solution of multiply layered cylinder. Finally, a lot of numerical examples are present.

Keywords: functionally graded materials; fundamental solution; transfer matrix method; multiply layered cylinder

1. Introduction

Many researchers studied the elasticity problem for the functionally graded composite materials (FGM). A lot of papers in this field were presented. In view of many literatures on the subject, we only study the problem for investigating the stress distribution in a thick cylinder of FGM. For a homogeneous hollow circular cylinder, the relevant elastic problem has been solved by (Muskhelishvili 1963, Timoshenko and Goodier 1970).

A lot of papers were devoted to study the stress distribution in thick-walled cylinder of FGM (Horgan and Chan 1999a, b, Zhang and Hasebe 1999, Shi *et al*. 2007, Tutuncu 2007, Dryden and Jayaraman 2006, Li and Peng 2009, Chen and Lin 2008). In an earlier year, a solution for the pressurized FGM hollow cylinder or disk problem was achieved (Horgan and Chan 1999a, b). It is assumed that the material and the thermal properties are varying along the radial direction with a power law function. It is shown that the stress response of the inhomogeneous cylinder is significantly different from that of the homogeneous body. For example, in contrast with the situation for the homogeneous material, the maximum hoop stress does not find along the inner surface. Some exact elastic solutions were developed for a radially nonhomogeneous hollow circular cylinder (Zhang and Hasebe 1999, Shi *et al*. 2007).

A problem for the thick-walled FGM cylinder was studied, which was reduced to an ordinary differential equation with respect to the radial displacement (Tutuncu 2007). Two types of Young's elastic modulus for evaluating stresses in pipes were suggested (Dryden and Jayaraman 2006).

The stress analysis for a functionally graded hollow cylinder was studied (Tutuncu and Temel 2009). In the paper, the Young's modulus and Poisson's ratio were arbitrary functions of the radial coordinate. The studied problem can be reduced to a two-point boundary value problem with a governing differential equation of variable coefficients, and can be solved by the complementary functions method (CFM). The CFM reduces the boundary value problem to an initial-value problem (IVP) which can be solved accurately by one of many efficient methods such as Runge–Kutta method.

Recently, a study for dealing with a FGM hollow cylinder was proposed, which is reduced to a solution of Fredholm integral equation (Li and Peng 2009). In addition, a numerical solution was suggested to solve the problem, which was based on a superposition of two particular initial problems (Chen and Lin 2008). In addition, some hollow sphere problems of FGM were solved (Eslami *et al*. 2005, You *et al*. 2005). A consistent solution for the fully elastic and viscoelastic deformations of rotating functionally graded hollow and solid cylinders was obtained (Zenkour *et al*. 2008).

In recent years, a lot of problems for FGM thick-walled cylinders under more complicated conditions were solved. Based on the surface elasticity theory of Gurtin-Murdoch, thermo-elastic fields within rotating nanoshafts with varying material properties subjected to a thermal field were explicitly examined. (Kiani 2016). A thick truncated hollow cone with finite length made of two-dimensional functionally graded materials subjected to combined loads as internal, external and axial pressure was considered (Asemi *et al*. 2011). The finite element method based on the Rayliegh-Ritz energy formulation was applied to obtain the elastic behavior of the functionally graded thick truncated cone.

Strain gradient elasticity formulation for analysis of FG

---

*Corresponding author, Professor
E-mail: chens@ujs.edu.cn

(functionally graded) micro-cylinders was presented (Sadeghia *et al.* 2012). The material properties are assumed to obey a power law in radial direction. The governing differential equation is derived as a fourth order ODE. An elasticity solution for the functionally graded thick-walled tube subjected to internal pressure was given in terms of volume fractions of constituents (Xin *et al.* 2014).

Airy stress function was employed to derive analytical solutions for plane strain static deformations of a functionally graded (FG) hollow circular cylinder with two elastic constants to be functions of the radius r (Nie and Batra 2010). In the study, the applied loading, for example, along the inner boundary are arbitrary. For a functionally graded (FG) circular cylinder loaded by uniform pressures on the inner and the outer surfaces and Young's modulus varying in the radial direction, Nie and Batra (2013) found the lower and upper bounds for Young's modulus of the energetically equivalent homogeneous cylinder.

A novel solution was provided for thick-walled cylinders made of functionally graded materials (Chen 2015). In the formulation, the cylinder was divided into N layers with constant elastic constant. A numerical solution for multiple confocal elliptic dissimilar cylinders was provided (Chen 2017). The medium is composed of many confocal elliptic dissimilar cylinders. The transfer matrix method is used to study the continuity condition for the stress and displacement along the interfaces.

In this paper, two fundamental solutions for FGM cylinder are proposed, which are obtained from the numerical solution of an ordinary differential equation. The two fundamental solutions are defined by two particular initial boundary conditions. By using the two fundamental solutions, the transfer matrix **N** can be formulated for the single layer case ($a \leq r \leq b$). The matrix gives a relation between the values of stress and displacement at the two end points, or $r = a$ and $r = b$. The transfer matrix method also provides an effective way for the solution of multiply layered cylinder. Several numerical results are presented. In the examples, the Young's modulus is assumed in the form: (a) $E(r) = E_o(1 + \beta s)$ or (b) $E^{(j)}(r) = E_o(\alpha_j + \beta_j s_j)$, $s_j = (r - a_j)/(b - a)$ $a_j \leq r \leq b_j$, (j=1,2,3) in the case of cylinder with three layers . We prove from the computed results that the influence of inhomogeneous Young's modulus to the stress distribution is significant.

2. Boundary value problem for single layer FGM cylinder with an arbitrary elastic property

In order to solve the boundary value problem (BVP) of a thick-walled FGM cylinder with general elastic response, we introduce an ordinary differential equation and the concept of transfer matrix. Based on the transfer matrix method, we provide a lot of examples and numerical solutions for FGM cylinder.

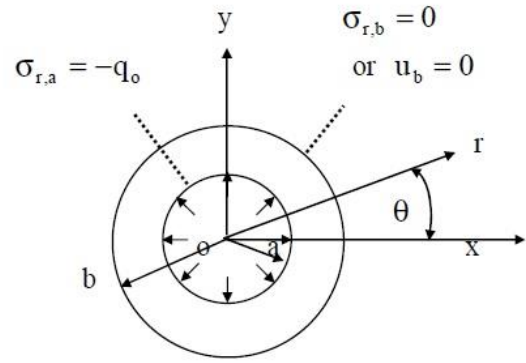*2.1 Formulation of ordinary differential equation for a thick cylinder made of functionally graded material*

Fig. 1 Two typical boundary conditions: (a) $\sigma_{r,a} = -q_o$ at r=a, $\sigma_{r,b} = 0$ at r=b and (b) $\sigma_{r,a} = -q_o$ at r=a, $u_b = 0$ at r=b

We investigate a long cylinder with inner radius "a" and outer radius "b" (Fig. 1). Along the inner boundary ($r = a$) and outer boundary ($r = b$) some traction or displacement boundary value conditions are assumed.

We study the problem in the polar coordinates (r, θ). In the symmetrical deformation case, the stress components σ_r and σ_θ should satisfy the following equilibrium equation (Timoshenko and Goodier 1970)

$$\frac{d\sigma_r}{dr} + \frac{\sigma_r - \sigma_\theta}{r} = 0 \qquad (1)$$

Now we introduce a function $F(r)$ and let

$$\sigma_r = \frac{F(r)}{r}, \qquad \sigma_\theta = \frac{dF}{dr} \qquad (2)$$

In this case, Eq. (1) can be satisfied automatically.

The displacement in the r-direction is denoted by "u". Two strain components can be expressed as (Muskhelishvili 1963, Timoshenko and Goodier 1970)

$$\varepsilon_r = \frac{du}{dr}, \quad \varepsilon_\theta = \frac{u}{r} \quad \text{(with } u = \varepsilon_\theta r \text{)} \qquad (3)$$

By using Eq. (3), we will obtain the following compatibility condition for displacement

$$\varepsilon_r = \frac{d(r\varepsilon_\theta)}{dr}, \quad \text{or} \quad \varepsilon_r = \varepsilon_\theta + r\frac{d\varepsilon_\theta}{dr} \qquad (4)$$

We assume that the Poisson's ratio takes a constant value $\nu = 0.3$ and the Young's modulus E(r) is an arbitrary function. From the stress-strain relation in the plane strain case, we have

$$\varepsilon_r = \frac{1 - \nu^2}{E(r)}(\sigma_r - \frac{\nu}{1-\nu}\sigma_\theta) = \frac{1-\nu^2}{E(r)}(\frac{F}{r} - \frac{\nu}{1-\nu}\frac{dF}{dr}) \qquad (5)$$

$$\varepsilon_\theta = \frac{1 - \nu^2}{E(r)}(\sigma_\theta - \frac{\nu}{1-\nu}\sigma_r) = \frac{1-\nu^2}{E(r)}(\frac{dF}{dr} - \frac{\nu}{1-\nu}\frac{F}{r}) \qquad (6)$$

$$u = \varepsilon_\theta r = \frac{(1-\nu^2)r}{E(r)} \left(\frac{dF}{dr} - \frac{\nu}{1-\nu} \frac{F}{r} \right) \tag{7}$$

Substituting Eqs. (5) and (6) into Eq. (4) yields

$$\frac{d^2F}{dr^2} + \frac{1}{r}\frac{dF}{dr} - \frac{F}{r^2} - \left(\frac{dF}{dr} - \frac{\nu}{1-\nu}\frac{F}{r} \right) \frac{1}{E(r)}\frac{dE(r)}{dr} = 0 \tag{8}$$

$$(\text{ or } \Lambda(F(r)) = 0)$$

We study the problem within the range $a \le r \le b$ and use the following notations

$$\sigma_{r,a} = \sigma_r \big|_{r=a}, \qquad u_a = u \big|_{r=a} \tag{9}$$

$$\sigma_{r,b} = \sigma_r \big|_{r=b}, \qquad u_b = u \big|_{r=b} \tag{10}$$

In Eqs. (9) and (10), $\sigma_{r,a}$, $\sigma_{r,b}$ denote the stress σ_r at $r = a$ or $r = b$, and u_a, u_b denote the displacement "u" at $r = a$ or $r = b$, respectively.

There are four possibilities to formulate the boundary problems for a single layer cylinder case. They are as follows

$$\sigma_{r,a} = f_1, \qquad \sigma_{r,b} = f_2 \tag{11a}$$

$$\sigma_{r,a} = f_1, \qquad u_b = g_2 \tag{11b}$$

$$u_a = g_1, \qquad \sigma_{r,b} = f_2 \tag{11c}$$

$$u_a = g_1, \qquad u_b = g_2 \tag{11d}$$

where f_1, f_2, g_1 and g_2 are values given beforehand.

2.2 Derivation of the transfer matrix

Obviously, if we assume the two initial values for $\sigma_{r,a}$ and u_a at $r = a$, we will have definite values for $\sigma_{r,b}$ and u_b at $r = b$ (Fig. 1). The relation between ($\sigma_{r,a}$, u_a) and ($\sigma_{r,b}$, u_b) can be expressed through a transfer matrix $\mathbf{N}$. The transfer matrix $\mathbf{N}$ is not only used to the single layer case but also to the multiply layered case.

From Eq. (8), we can introduce the two fundamental functions $s_1(r)$ and $s_2(r)$ as follows

$$\Lambda(s_1(r)) = 0, \quad s_1 \big|_{r=a} = 1, \quad \frac{ds_1}{dr} \big|_{r=a} = 0, \tag{12}$$

(the first fundamental function)

$$\Lambda(s_2(r)) = 0, \quad s_2 \big|_{r=a} = 0, \quad \frac{ds_2}{dr} \big|_{r=a} = 1, \tag{13}$$

(the second fundamental function)

Clearly, it is easy to evaluate the numerical solution for Eq. (8) under the boundary condition Eq. (12) or (13) by using the Runge–Kutta method (Hildebrand 1974).

In fact, we can express the general solution for the ordinary differential equation Eq. (8), or $\Lambda(F(r)) = 0$, as follows

$$F(r) = c_1 s_1(r) + c_2 s_2(r) \tag{14a}$$

From Eqs. (12) and (13), we see that

$$F \big|_{r=a} = c_1, \quad \frac{dF}{dr} \big|_{r=a} = c_2 \tag{14b}$$

Clearly, the general solution $F(r) = c_1 s_1(r) + c_2 s_2(r)$ is a solution of Eq. (8) under the two initial boundary conditions $F \big|_{r=a} = c_1$, $\frac{dF}{dr} \big|_{r=a} = c_2$, where c_1 and c_2 are two undetermined coefficients. Further, the involved two coefficients c_1 and c_2 can be evaluated by the two boundary conditions shown by Eqs. (11a)- (11c) or (11d).

From the above-mentioned derivation, we can convert the boundary value problem into initial boundary value problem. We use the stress function method in the derivation. This method was suggested early by Tutuncu and Temel (2009). They called the method with the name of the complementary functions method (CFM). In addition, they chose the displacement as unknown function in the derivation.

In addition, from Eqs. (2), (7), (12), (13) and (14), we have

$$\sigma_{r,a} = c_1 \frac{s_1(r)}{r} \big|_{r=a} + c_2 \frac{s_2(r)}{r} \big|_{r=a} = \frac{1}{a}c_1$$

$$u_a = c_1 \frac{(1-\nu^2)a}{E(a)}\left(\frac{ds_1(r)}{dr} - \frac{\nu}{1-\nu}\frac{s_1(r)}{r} \right)\bigg|_{r=a}$$

$$+ c_2 \frac{(1-\nu^2)a}{E(a)}\left(\frac{ds_2(r)}{dr} - \frac{\nu}{1-\nu}\frac{s_2(r)}{r} \right)\bigg|_{r=a} \tag{15}$$

$$= \frac{(1-\nu^2)a}{E(a)}\left(-\frac{\nu}{(1-\nu)a}c_1 + c_2 \right) \tag{16}$$

Note that, in the derivation of Eqs. (15) and (16), we use the conditions $s_1 \big|_{r=a} = 1$, $ds_1/dr \big|_{r=a} = 0$, $s_2 \big|_{r=a} = 0$ and $ds_2/dr \big|_{r=a} = 1$ defined by Eqs. (12) and (13).

Eqs. (15) and (16) can be rewritten as

$$c_1 = a\sigma_{r,a}, \qquad c_2 = \frac{\nu}{1-\nu}\sigma_{r,a} + \frac{E(a)}{(1-\nu^2)a}u_a \tag{17}$$

or in a matrix form

$$\{\mathbf{c_1}\ \mathbf{c_2}\}^{\mathbf{T}} = \mathbf{H}\{\mathbf{\sigma_{r,a}}\ \mathbf{u_a}\}^{\mathbf{T}} \tag{18}$$

where

$$H_{11} = a, \quad H_{12} = 0, \quad H_{21} = \frac{v}{1-v},$$

$$H_{22} = \frac{E(a)}{(1-v^2)a} \tag{19}$$

Similarly, from Eqs. (12)-(14), we have

$$\sigma_{r,b} = c_1 \frac{s_1(r)}{r}\Big|_{r=b} + c_2 \frac{s_2(r)}{r}\Big|_{r=b} \tag{20}$$

$$u_b = c_1 \frac{(1-v^2)b}{E(b)}\left(\frac{ds_1(r)}{dr} - \frac{v}{1-v}\frac{s_1(r)}{r}\right)\Big|_{r=b}$$
$$+ c_2 \frac{(1-v^2)b}{E(b)}\left(\frac{ds_2(r)}{dr} - \frac{v}{1-v}\frac{s_2(r)}{r}\right)\Big|_{r=b} \tag{21}$$

Eqs. (20) and (21) may be written as

$$\sigma_{r,b} = \sigma_{r,b}^{1*}c_1 + \sigma_{r,b}^{2*}c_2, \quad u_b = u_b^{1*}c_1 + u_b^{2*}c_2 \tag{22}$$

where

$$\sigma_{r,b}^{1*} = \frac{s_1(r)}{r}\Big|_{r=b} = \frac{s_1(b)}{b},$$

$$u_b^{1*} = \frac{(1-v^2)b}{E(b)}\left(\frac{ds_1(r)}{dr} - \frac{v}{1-v}\frac{s_1(r)}{r}\right)\Big|_{r=b},$$

$$\sigma_{r,b}^{2*} = \frac{s_2(r)}{r}\Big|_{r=b} = \frac{s_2(b)}{b}, \tag{23}$$

$$u_b^{2*} = \frac{(1-v^2)b}{E(b)}\left(\frac{ds_2(r)}{dr} - \frac{v}{1-v}\frac{s_2(r)}{r}\right)\Big|_{r=b}$$

Note that, after numerical integration for two fundamental solutions defined by Eqs. (12) and (13), the four values $\sigma_{r,b}^{1*}$, u_b^{1*}, $\sigma_{r,b}^{2*}$ and u_b^{2*} can be evaluated accordingly.

Eq. (22) can be rewritten in a matrix form

$$\{\mathbf{\sigma_{r,b}}\ \mathbf{u_b}\}^{\mathbf{T}} = \mathbf{G}\{\mathbf{c_1}\ \mathbf{c_2}\}^{\mathbf{T}} \tag{24}$$

where

$$G_{11} = \sigma_{r,b}^{1*}, \quad G_{12} = \sigma_{r,b}^{2*}, \quad G_{21} = u_b^{1*}, \quad G_{22} = u_b^{2*} \tag{25}$$

By using Eqs. (18) and (24), we have

$$\{\mathbf{\sigma_{r,b}}\ \mathbf{u_b}\}^{\mathbf{T}} = \mathbf{N}\{\mathbf{\sigma_{r,a}}\ \mathbf{u_a}\}^{\mathbf{T}} \tag{26}$$

where the matrix $\mathbf{N}$ is defined by

$$\mathbf{N} = \mathbf{GH} \tag{27}$$

The matrix $\mathbf{N}$ is called the transfer matrix in this paper, which gives a relation between the vector $\{\mathbf{\sigma_{r,b}}\ \mathbf{u_b}\}^{\mathbf{T}}$ to

vector $\{\mathbf{\sigma_{r,a}}\ \mathbf{u_a}\}^{\mathbf{T}}$.

In the first example, we want to solve the following BVP

$$\sigma_{r,a} = \sigma_r\Big|_{r=a} = -q_o, \sigma_{r,b} = \sigma_r\Big|_{r=b} = 0 \tag{28}$$

In fact, one relation in Eq. (26) can be expressed as

$$\sigma_{r,b} = N_{11}\sigma_{r,a} + N_{12}u_a \tag{29}$$

By using Eqs. (28) and (29), we will find

$$u_a = N_{11}q_o / N_{12} \tag{30}$$

Since the value $\sigma_{r,a} = -q_o$ is given beforehand and the value u_a can be evaluated from Eq. (30), two values c_1 and c_2 can be obtained by using Eq. (18). Finally, the function $F(r) = c_1 s_1(r) + c_2 s_2(r)$ shown by Eq. (14) is obtained. Thus, the whole stress field for the single layer cylinder is obtainable.

In the second example, we want to solve the following BVP

$$\sigma_{r,a} = \sigma_r\Big|_{r=a} = -q_o, \quad u_b = u\Big|_{r=b} = 0 \tag{31}$$

In this case, one needs to use the following relation in Eq. (26)

$$u_b = N_{21}\sigma_{r,a} + N_{22}u_a \tag{32}$$

By using Eqs. (31) and (32), we find

$$u_a = N_{21}q_o / N_{22} \tag{33}$$

The next steps are same as in the first example.

2.3 Numerical solution in the single layer case

Several boundary value problems are introduced below.
Example 1
In the first example (Fig. 1), we assume the Young's modulus as follows

$$E(r) = E_o(1 + \beta s) \quad \text{where} \quad s = \frac{r-a}{b-a}$$
$$(\text{with} \quad E(a) = E_o, \quad E(b) = (\beta+1)E_o) \tag{34}$$

Note that, the Young's modulus changes from $E(a) = E_o$ ($r = a$) to $E(b) = (\beta+1)E_o$ ($r = b$), and $\beta = 0$ represents the homogeneous case.

The cylinder is applied by an inner pressure q_o and the boundary conditions take the following form (Fig. 1)

$$\sigma_{r,a} = \sigma_r\Big|_{r=a} = -q_o, \quad \sigma_{r,b} = \sigma_r\Big|_{r=b} = 0 \tag{35}$$

Now we may summarize necessary steps of solution as follows: (a) to evaluate numerically two fundamental solutions $s_1(r)$ and $s_2(r)$ defined by Eqs. (12) and (13), (b) to obtain three matrices $\mathbf{H}$, $\mathbf{G}$ and $\mathbf{N}$ by their definition shown by Eqs. (18), (19), (24), (25) and (27), (c) to evaluate u_a by using Eq. (30) and (d) to evaluate two constant c_1

and c_2 from $\sigma_{r,a}$ ($=-q_o$) and u_a by using Eq. (18). Thus the whole stress field is obtained from Eq. (14).

In the solution of the differential equation, we use N=200 divisions in the integration (Hildebrand 1974). The calculated results for stresses can be expressed as

$$\sigma_r = f_1(\beta,r)q_o, \qquad \sigma_\theta = f_2(\beta,r)q_o,$$

$$\sigma_e = \sigma_\theta - \sigma_r = f_3(\beta,r)q_o, \tag{36}$$

The calculated results for f_1, f_2, f_3, under the conditions: (a) $a/b = 0.5$, and (b) $\beta = 0$, 1,2,3 and 4, are plotted in Figs 2-4, respectively. Clearly, for $\beta = 0$, 1,2,3 and 4, we have $E(b)/E(a) = 1$, 2, 3, 4 and 5, respectively, and $\beta = 0$ represents the homogeneous case.

We see from general theory of strength of materials that the strength of the cylinder mainly depends on the stress component $\sigma_e = \sigma_\theta - \sigma_r$ (or $f_3(\beta,r)$). From Fig. 4 we see that the σ_e distribution along the interval ($a \leq r \leq b$) is varying rapidly in the homogeneous material case. For example, in the case of $\beta = 0$, we have $f_3 = 2.6667$, 1.1852 and 0.6667, for $(r-a)/(b-a)$ =0, 0.5 and 1.0, respectively. In addition, a higher β value can considerably improve the σ_e distribution along the interval ($a \leq r \leq b$). For example, at $\beta = 4$, we have $f_3 = 1.4710$, 1.4435 and 1.2977, for $(r-a)/(b-a)$ =0, 0.5 and 1.0, respectively. This means that if outer portion of the cylinder is more rigid, the safe condition is better. On contrary, if outer portion of the cylinder is less rigid, the safe condition becomes worse (see the curves for $\beta = 0$ or $\beta = 1$ in Fig. 4).
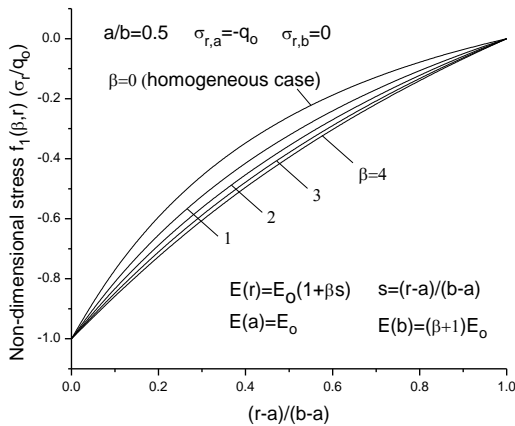

Fig. 2 Non-dimensional radial stress $f_1(\beta,r)$, for the σ_r component in cylinder, with a/b=0.5, $E(r) = E_o(1 + \beta s)$, s=(r-a)/(b-a) and $\sigma_{r,a} = -q_o$, $\sigma_{r,b} = 0$ (see Eq. (36) and Fig. 1)
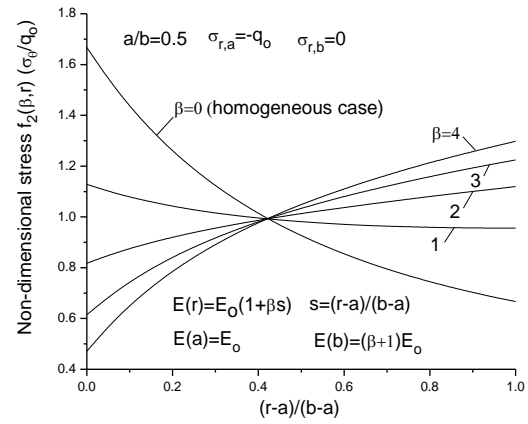

Fig. 3 Non-dimensional circumferential stress $f_2(\beta,r)$, for the σ_θ component in cylinder, with a/b=0.5, $E(r) = E_o(1 + \beta s)$, s=(r-a)/(b-a) and $\sigma_{r,a} = -q_o$, $\sigma_{r,b} = 0$ (see Eq. (36) and Fig. 1)
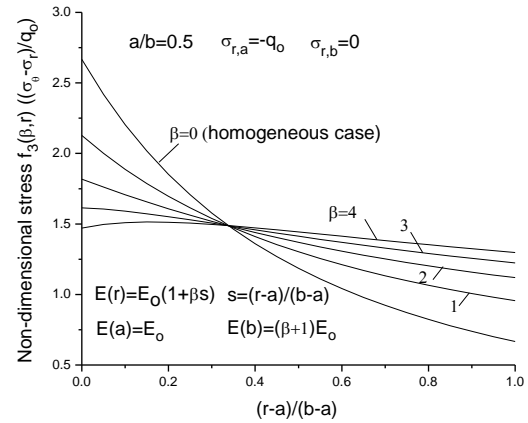

Fig. 4 Non-dimensional stress $f_3(\beta,r)$, for the $\sigma_e = \sigma_\theta - \sigma_r$ component in cylinder, with a/b=0.5, $E(r) = E_o(1 + \beta s)$, s=(r-a)/(b-a) and $\sigma_{r,a} = -q_o$, $\sigma_{r,b} = 0$ (see Eq. (36) and Fig. 1)

Example 2

In the second example, the Young's modulus still takes the form shown by Eq. (34). The cylinder is subjected to an inner pressure q_o and the outer boundary is fixed. Thus, the boundary conditions take the following form (Fig. 1)

$$\sigma_{r,a} = \sigma_r \big|_{r=a} = -q_o, \quad u_b = u \big|_{r=b} = 0 \tag{37}$$

The other conditions are same as in the first example.

The calculated results for stresses are still expressed by Eq. (36). The calculated results for f_1, f_2, f_3, under the conditions: (a) $a/b = 0.5$, and (b) $\beta = 0$, 1,2,3 and 4, are plotted in Figs. 5-7, respectively.

It is seen from Fig. 7 that the condition of $\beta = 4$ can provide a better distribution for σ_e component. In fact, in the homogenous case (or $\beta = 0$), we have $\sigma_e = 1.2308$ (at r = a), and $\sigma_e = 0.3077$ (at r = b). Thus, the ratio $\sigma_e\mid_{r=b} / \sigma_e\mid_{r=a} = 0.25$ (=0.3077/1.2308, or 25%) is achieved. That is to say the outer boundary has too much safety factor when σ_e at the inner boundary point reaches its limit value.
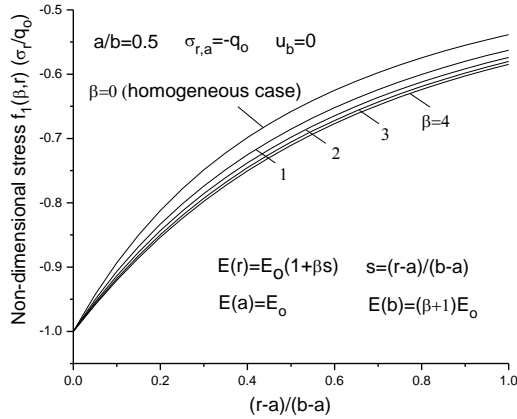

Fig. 5 Non-dimensional radial stress $f_1(\beta, r)$, for the σ_r component in cylinder, with a/b=0.5, $E(r) = E_o(1 + \beta s)$, s=(r-a)/(b-a) and $\sigma_{r,a} = -q_o$, $u_b = 0$ (see Eq. (36) and Fig. 1)
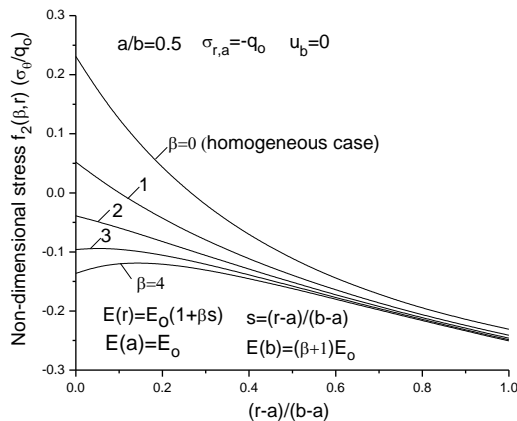

Fig. 6 Non-dimensional circumferential stress $f_2(\beta, r)$, for the σ_θ component in cylinder, with a/b=0.5, $E(r) = E_o(1 + \beta s)$, s=(r-a)/(b-a) and $\sigma_{r,a} = -q_o$, $u_b = 0$ (see Eq. (36) and Fig. 1)
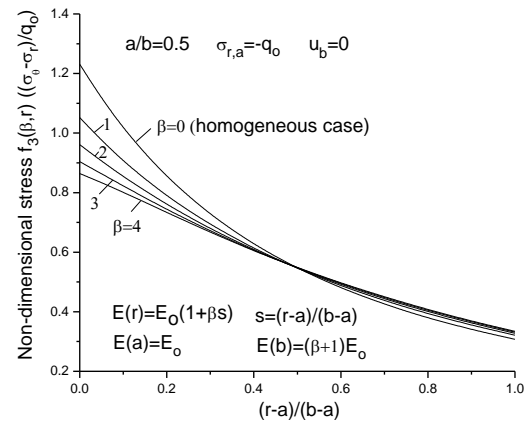

Fig. 7 Non-dimensional stress $f_3(\beta, r)$, for the $\sigma_e = \sigma_\theta - \sigma_r$ component in cylinder, with a/b=0.5, $E(r) = E_o(1 + \beta s)$, s=(r-a)/(b-a) and $\sigma_{r,a} = -q_o$, $u_b = 0$ (see Eq. (36) and Fig. 1)

However, under condition of $\beta = 4$, we have $\sigma_e = 0.8640$ (at r=a), and $\sigma_e = 0.3341$ (at r=b). In this case, the relative ratio is $\sigma_e\mid_{r=b} / \sigma_e\mid_{r=a} = 0.3867$ (=0.3341/0.8640).

However, in the second example, the improvement for σ_e component is not as much as in the first example. For example, in the case of $\beta = 4$, we have $\sigma_e\mid_{r=b} / \sigma_e\mid_{r=a} = 0.8822$ and 0.3867 in the first and second examples respectively, which can be seen from Figs. 4 and 7.

3. Solution for multiply layered cylinder using the transfer matrix method

As mentioned previously, the transfer matrix N gives the relation of (σ_r, u) at the initial point (r=a) to those at the end point (r=b). For the problem of multiply layered cylinder, we can propose many transfer matrices $\mathbf{N}^{(j)}$ (j=1,2,). By linking those transfer matrices from the continuity condition along the interfaces and using the assumed boundary conditions, we can solve the boundary value problem for the multiply layered cylinder.

3.1 Procedure for the solution of multiply layered cylinder using the transfer matrix method

We study the problem for a cylinder with three layers (Fig. 8). The cylinder is composed of three layers along the intervals $a_j \leq r \leq b_j$ (j=1,2,3), where $a_1 = a$, $a_2 = b_1 = (2a+b)/3$, $a_3 = b_2 = (a+2b)/3$ and $b_3 = b$ (Fig. 8). We choose the Young's elastic modulus for three layers as follows

$$E^{(j)}(r) = E_o(\alpha_j + \beta_j s_j) \ , \qquad s_j = \frac{r - a_j}{b - a} \ ,$$

$$a_j \le r \le b_j \ , \quad (j=1,2,3) \tag{38}$$

where α_j, β_j (j=1,2,3) are given beforehand.

In the derivation, we denote the boundary values at the initial point for j-th layer (j=1,2,3)   by $\sigma_{r,in}^{(j)}$, $u_{in}^{(j)}$, and at the end point by $\sigma_{r,end}^{(j)}$ $u_{end}^{(j)}$ (j=1,2,3) (Fig. 8). Clearly, the continuity condition between layers can be expressed as

$$\sigma_{r,end}^{(j)} = \sigma_{r,in}^{(j+1)}, \quad u_{end}^{(j)} = u_{in}^{(j+1)}, \quad (j=1,2) \tag{39}$$

In addition, we denote the relevant matrices by $\mathbf{H}^{(j)}$, $\mathbf{G}^{(j)}, \mathbf{N}^{(j)}$ (j=1,2,3) (refer to Eqs. (18), (19), (24), (25), (27)), and denote the relevant coefficients before the fundamental solutions by $c_1^{(j)}$, $c_2^{(j)}$ (refer to Eq. (14)).

By using the result obtained in the single layer case, or from Eqs. (26) and (39), we have

$$\{\sigma_{r,in}^{(j+1)} \mathbf{u}_{in}^{(j+1)}\}^{\mathbf{T}} = \{\sigma_{r,end}^{(j)} \mathbf{u}_{end}^{(j)}\}^{\mathbf{T}} = \mathbf{N}^{(j)} \{\sigma_{r,in}^{(j)} \mathbf{u}_{in}^{(j)}\}^{\mathbf{T}} \ ,$$

$$(j=1,2) \tag{40}$$

$$\{\sigma_{r,end}^{(3)} \mathbf{u}_{end}^{(3)}\}^{\mathbf{T}} = \mathbf{N}^{(3)} \{\sigma_{r,in}^{(3)} \mathbf{u}_{in}^{(3)}\}^{\mathbf{T}} \tag{41}$$

In Eqs. (40) and (41), there are eight unknowns, namely, $\sigma_{r,in}^{(1)}$, $\mathbf{u}_{in}^{(1)}$, $\sigma_{r,in}^{(2)}$, $\mathbf{u}_{in}^{(2)}$, $\sigma_{r,in}^{(3)}$, $\mathbf{u}_{in}^{(3)}$, $\sigma_{r,end}^{(3)}$ and $\mathbf{u}_{end}^{(3)}$ in six simultaneous equations.
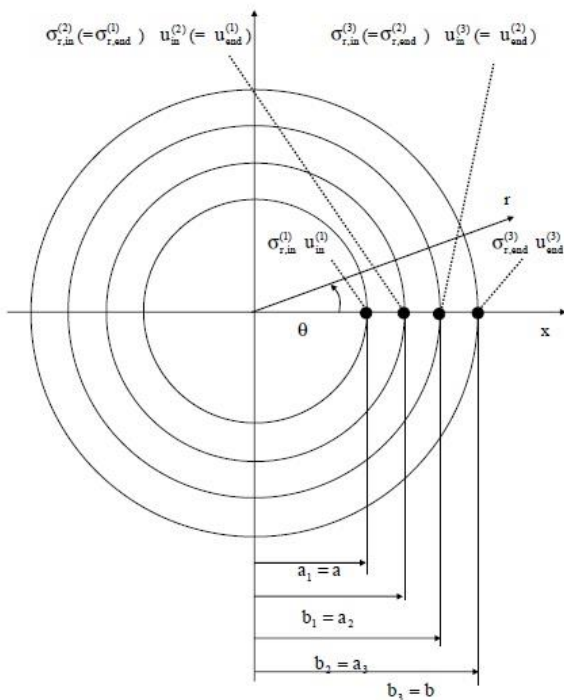

Fig. 8 A cylinder with three layers

When the three layers cylinder is applied by an inner pressure with intensity q_o (at $r = a_1 = a$) and the outer boundary is traction free (at $r = b_3 = b$), the following boundary value problem is formulated

$$\sigma_{r,in}^{(1)} = -q_o \ , \qquad \sigma_{r,end}^{(3)} = 0 \ ,$$

$$(\text{or } \sigma_{r,a} = -q_o \ , \qquad \sigma_{r,b} = 0) \tag{42}$$

Clearly, substituting Eq. (42) into Eqs. (40) and (41), we can obtain the other six unknowns $\mathbf{u}_{in}^{(1)}$, $\sigma_{r,in}^{(2)}$, $\mathbf{u}_{in}^{(2)}$, $\sigma_{r,in}^{(3)}$, $\mathbf{u}_{in}^{(3)}$ and $\mathbf{u}_{end}^{(3)}$ from the system of the algebraic equations. As mentioned previously, once $\sigma_{r,in}^{(1)}$, $\mathbf{u}_{in}^{(1)}$, $\sigma_{r,in}^{(2)}$, $\mathbf{u}_{in}^{(2)}$, $\sigma_{r,in}^{(3)}$, $\mathbf{u}_{in}^{(3)}$ are obtained, the stress distribution for all layers are obtainable.

3.2 Numerical example for three layers cylinder

Example 3

In the present example, the case for the three layered cylinder is considered   and the Young's elastic modulus is assumed as

$$E^{(1)}(r) = E_o(1 + 4(1 - \gamma)s_1) \ ,$$

$$s_1 = \frac{r - a_1}{b - a} \qquad (a_1 \le r \le b_1) \tag{43a}$$

$$E^{(2)}(r) = E_o(1 + \frac{4(1 - \gamma)}{3} + 4s_2) \ ,$$

$$s_2 = \frac{r - a_2}{b - a} \qquad (a_2 \le r \le b_2) \tag{43b}$$

$$E^{(3)}(r) = E_o(1 + \frac{4(2 - \gamma)}{3} + 4(1 + \gamma)s_3) \ ,$$

$$s_3 = \frac{r - a_3}{b - a} \qquad (a_3 \le r \le b_3) \tag{43c}$$

wher $a_1 = a$, $a_2 = b_1 = (2a + b)/3$, $a_3 = b_2 = (a + 2b)/3$ and $b_3 = b$. In Eq. (43), the factor γ represents a modification to the case shown by Eq. (34) with β =4. Clearly, in any given value of γ, $E(b)/E(a) = 5$.

The function is expressed alternatively by

$$E(r) = h_E(\gamma, r)E_o \tag{44}$$

For some given values of γ (=-0.5, -0.25, 0, 0.25, 0.5), the function $h_E(\gamma, r)$ is plotted in Fig. 9.

In this example, the boundary conditions take the following form $\sigma_{r,a} = \sigma_r \big|_{r=a} = -q_o$, $\sigma_{r,b} = \sigma_r \big|_{r=b} = 0$, which was   shown by Eq. (28) previously. The calculated results for stresses can be expressed as
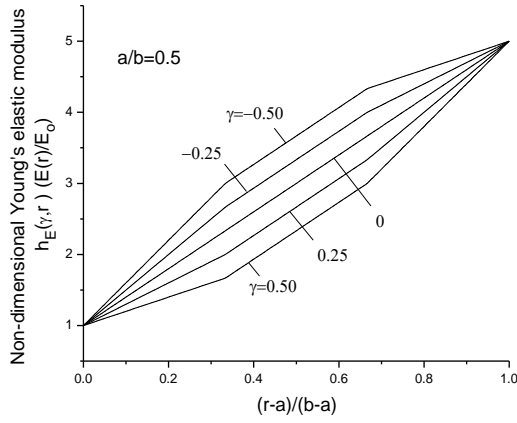
Fig. 9 Non-dimensional Young's modulus $h_E(\gamma,r)$ (= $E(r)/E_o$)), in a three layered cylinder (see Eqs. (41) and (44))
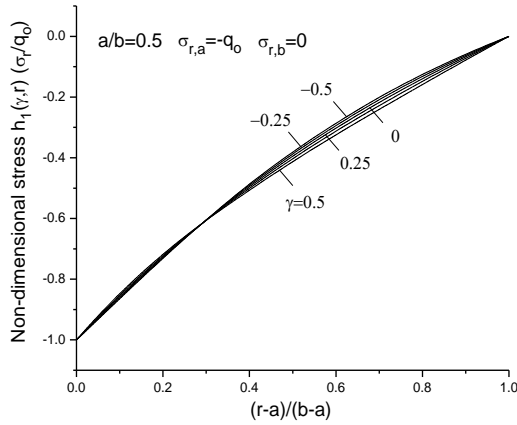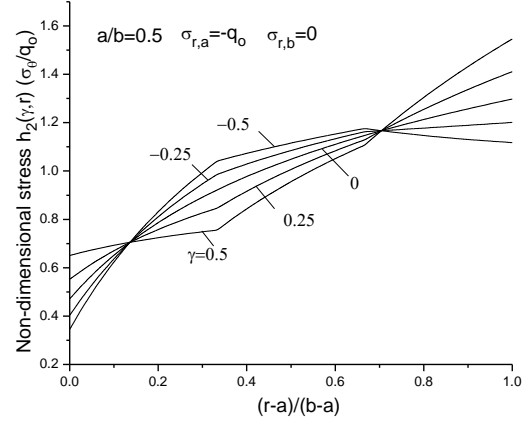

Fig. 11 Non-dimensional circumferential stress $h_2(\gamma,r)$, for the σ_θ component in a three layered cylinder, with a/b=0.5 and $\sigma_{r,a}=-q_o$, $\sigma_{r,b}=0$ (see Eq. (45) and Fig. 5)

Fig. 10 Non-dimensional radial stress $h_1(\gamma,r)$, for the σ_r component in a three layered cylinder, with a/b=0.5 and $\sigma_{r,a}=-q_o$, $\sigma_{r,b}=0$ (see Eqs. (45))

$$\sigma_r = h_1(\gamma,r)q_o, \qquad \sigma_\theta = h_2(\gamma,r)q_o$$
$$\sigma_e = \sigma_\theta - \sigma_r = h_3(\gamma,r)q_o \qquad (45)$$

The calculated results for h_1, h_2, h_3, under the conditions: (a) $a/b = 0.5$, and (b) γ =-0.5, -0.25, 0, 0.25 and 0.5, five cases, are plotted in Figs. 10-12, respectively.

Taking $\gamma = -0.5$ as an example, the derivatives $dE(r)/dr$ take the values $6E_o/(b-a)$, $4E_o/(b-a)$, $2E_o/(b-a)$, for the first, second and third layer, respectively. In this case, the function E(r) is continuous at $r = a_j$ (j=1,2), but the derivative $dE(r)/dr$ is discontinuous at $r = a_j$ (j=1,2) (see Fig. 9). In this case, the stress component $h_3(\gamma,r)$, for example at $\gamma = -0.5$, has a
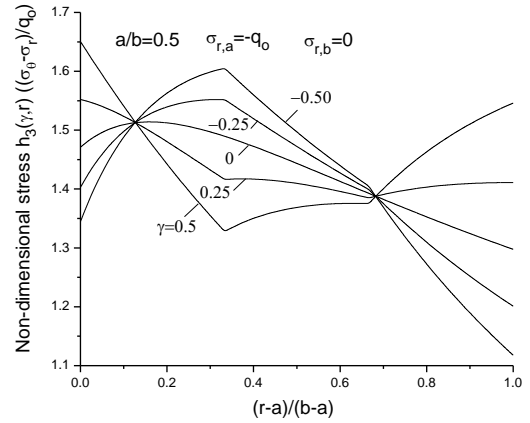

Fig. 12 Non-dimensional stress $h_3(\gamma,r)$, for the $\sigma_e = \sigma_\theta - \sigma_r$ component in a three layered cylinder, with a/b=0.5 and $\sigma_{r,a}=-q_o$, $\sigma_{r,b}=0$ (see Eq. (45) and Fig. 5)

broken configuration, which is worse than its counterpart in the smooth case of E(r) (see Figs. 4 and 12). It is seen from Fig. 12 that the case of $\gamma = 0$ still provides better stress distribution for the stress component $\sigma_e (= h_3(\gamma,r)q_o)$.

4. Conclusions

Some researchers try to find a solution for cylinders of FGM in a closed form. However, this goal can be achieved only in some simpler case. Clearly, for the cases of the arbitrary elastic response, one needs to develop some numerical technique. The suggested transfer matrix method

provides an effective way for the addressed problem. The technique meanly depends on the two fundamental solutions defined by Eqs. (12) and (13), and the transfer matrix can be formulated simply by using results obtained in the two fundamental solutions. For the single layer case, one only needs to substitute the boundary conditions into the equations derived from transfer matrix. Similarly, the transfer matrix method also provides a powerful tool for the solution of multiply layer case.

The adopted Young's modulus has significant influence to the stress distribution in the cylinders of FGM. From the general theory of strength of materials, the smooth distribution of the stress component σ_e ($\sigma_\theta - \sigma_r$) is desirable in design. From Fig. 4 we see that in the case of $\beta = 4$ in the Young's modulus $E(r) = E_o(1 + \beta s)$ (where $s = (r - a)/(b - a)$), the σ_e distribution is better among many options.

References

Asemi, K., Salehi, M. and Akhlaghi, M. (2011), "Elastic solution of a two-dimensional functionally graded thick truncated cone with finite length under hydrostatic combined loads", *Acta Mech.*, **217**(1-2), 119-134.

Chen, Y.Z. (2015), "A novel solution for thick-walled cylinders made of functionally graded materials", *Smart Struct. Syst.*, **15**(6), 1503-1520.

Chen, Y.Z. (2017), "Numerical solution for multiple confocal elliptic dissimilar cylinders", *Smart Struct. Syst.*, **19**(2), 203-211.

Chen, Y.Z. and Lin, X.Y. (2008), "Elastic analysis for thick cylinders and spherical pressure vessels made of functionally graded materials", *Comput. Mater. Sci.*, **44**(2), 581-587.

Dryden, J. and Jayaraman, K. (2006), "Effect of inhomogeneity on the stress in pipes", *J. Elasticity*, **83**(2), 179-189.

Eslami, M.R., Babaei, M.H. and Poultangari, R. (2005), "Thermal and mechanical stresses in a functionally graded thick sphere", *Int. J. Pres. Ves. Pip.*, **82**(7), 522-527.

Hildebrand, F.B. (1974), *Introduction to Numerical Analysis* (McGraw-Hill, New York)

Horgan, C.O. and Chan, A.M. (1999a), "The pressurized hollow cylinder or disk problem for functionally graded isotropic linearly elastic materials", *J. Elasticity*, **55**(1), 43-59.

Horgan, C.O. and Chan, A.M. (1999b), "The stress response of functionally graded isotropic linearly elastic rotating disks", *J. Elasticity*, **55**(3), 219-230.

Kiani, K. (2016), "Stress analysis of thermally affected rotating nanoshafts with varying material properties", *Acta Mech. Sinica*, **32**(5), 813-827.

Li, X.F. and Peng, X.L. (2009), "A pressurized functionally graded hollow cylinder with arbitrarily varying material properties", *J. Elasticity*, **96**(1), 81-95.

Muskhelishvili, N.I. (1963), *Some Basic Problems of the Mathematical Theory of Elasticity*, Noordhoff, Groningen.

Nie, G.J. and Batra, R.C. (2010), "Exact solutions and material tailoring for functionally graded hollow circular cylinders", *J Elasticity*, **99**(2), 179-201.

Nie, G.J. and Batra, R. C. (2013), "Optimum Young's modulus of a homogeneous cylinder energetically equivalent to a functionally graded cylinder", *J. Elasticity*, **110**(1), 95-110.

Sadeghia, H., Baghani, M. and Naghdabadi, R. (2012), "Strain gradient elasticity solution for functionally graded micro-cylinders", *Int. Eng. Sci.*, **50**(1), 22-30.

Shi, Z.F., Zhang, T.T. and Xiang, H.J. (2007), "Exact solutions of heterogeneous elastic hollow cylinders", *Comput. Struct.*, **79**(1), 140-147.

Timoshenko, S.P. and Goodier, J.N. (1970), *Theory of Elasticity* (McGraw-Hill, New York).

Tutuncu, N. (2007), "Stresses in thick-walled FGM cylinders with exponentially-varying properties", *Eng. Struct.*, **29**(9), 2032-2035.

Tutuncu, N. and Temel, B. (2009), "A novel approach to stress analysis of pressurized FGM cylinders, disks and spheres", *Comp. Struct.*, **91**(3), 385-390.

Xin, L.B., Dui, G.S., Yang, S.Y. and Zhang, J.M. (2014), "An elasticity solution for functionally graded thick-walled tube subjected to internal pressure ", *Int. J. Mech. Sci.*, **89**, 344-349.

You, L.H., Zhang, L.L. and You, X.Y. (2005), "Elastic analysis of internally pressurized thick-walled spherical pressure vessels of functionally graded materials", *Int. J. Pres. Ves. Pip.*, **82**(5), 347-354.

Zenkour, A.M., Elsibai, K.A. and Mashat, D.S. (2008), "Elastic and viscoelastic solutions to rotating functionally graded hollow and solid cylinders", *Appl. Math. Mech.*, **29**(12), 1601-1616.

Zhang, X. and Hasebe, N. (1999), "Elasticity solution for a radially nonhomogeneous hollow circular cylinder", *J. Appl. Mech.*, **66**(3), 598-606.

CC